energies

MDPI

Article

Combined Radiative Cooling and Solar Thermal Collection: Experimental Proof of Concept

Sergi Vall, Marc Medrano, Cristian Solé and Albert Castell *

Sustainaible Energy, Machinery and Buildings (SEMB) Research Group, INSPIRES Research Centre, Universitat de Lleida, Pere de Cabrera s/n, 25001 Lleida, Spain; svall@diei.udl.cat (S.V.); mmedrano@diei.udl.cat (M.M.); csole@diei.udl.cat (C.S.)

* Correspondence: acastell@diei.udl.cat

Received: 29 December 2019; Accepted: 14 February 2020; Published: 18 February 2020

Abstract: Climate change is becoming more important day after day. The main actor to decarbonize the economy is the building stock, especially in the energy used for Domestic Hot Water (DHW), heating and cooling. The use of renewable energy sources to cover space conditioning and DHW demands is growing every year. While solar thermal energy can cover building heating and DHW demands, there is no technology with such potential and development for space cooling. In this paper, a new concept of combining radiative cooling and solar thermal collection, the Radiative Collector and Emitter (RCE), through the idea of an adaptive cover, which uses different material properties for each functionality, is for the first time experimentally tested and proved. The RCE relies on an adaptive cover that uses different material properties for each functionality: high spectral transmittance in the solar radiation band and very low spectral transmittance in the infrared band during solar collection mode, and high spectral transmittance in the atmospheric window wavelength during radiative cooling mode. Experiments were performed during the summer period in Lleida (Dry Mediterranean Continental climate). The concept was proved, demonstrating the potential of the RCE to heat up water during daylight hours and to cool down water during the night. Daily/nightly average efficiencies up to 49% and 32% were achieved for solar collection and radiative cooling, respectively.

Keywords: radiative cooling; solar thermal collection; renewable energy; low-grade energy source; building integration; experimental setup

1. Introduction

The effects of climate change are becoming more dangerous and destructive day after day. This subject is in the public eye and governments are taking actions on this matter. To mitigate or reverse these effects, long-term greenhouse gas emissions goals are being set. One of the main actors to decarbonize the economy is the building stock, responsible for 36% of all CO_2 emissions in the EU. Special consideration must be taken in the energy used for heating and cooling which is up to 50% of the final energy consumption (80% of which in buildings). This is why special efforts are being made in renovating the current building stock by energy efficiency means as well as considering the deployment of renewables [1].

The use of renewable energy sources to cover space conditioning and Domestic Hot Water (DHW) demands seems more likely over the years. While solar thermal energy can cover building heating and DHW demands [2], there is not yet a technology with such potential and development for space cooling. In fact, despite the existence of a few renewable cooling technologies, they present significant limitations [3].

Compression and absorption heat pumps are the main technologies for cooling purposes, compression heat pumps being the most common. These devices consume large amounts of electricity,

although they are considered renewable sources under certain circumstances [4,5]. On the other hand, absorption heat pumps may use solar energy as driving heat, but they present some important disadvantages such as, low efficiency, a need of high temperatures (>100 °C), large equipment sizes and the need for auxiliary equipment such as a cooling tower (which increases the cost of the installation and can result in health problems such as legionella) [6].

Alternatively, radiative cooling is a renewable cooling technology that can complement conventional cooling systems. Radiative cooling uses the sky as a heat sink, benefiting from its effective temperature which is much lower than ambient temperature. Energy can be dissipated to the sky taking advantage of the infrared atmospheric window (7–14 μm). This window allows infrared radiation to pass directly to outer space without intermediate absorption and re-emission in the atmosphere. Heat dissipation is produced by longwave radiation (thermal radiation) from a surface to the sky. The sky temperature during the night can be lower than 0 °C or even −10 °C [7], allowing temperatures suitable for cooling. However, this phenomenon is a priori only valid during the night, since during the day solar radiation (shortwave radiation) is higher and the radiation balance results in thermal gains (heating). The sky temperature can be related to the ambient temperature using sky emissivity [8].

Radiative cooling technology attracted a lot of attention in the 1970s, with lots of papers published. However, the lack of suitable materials and solutions in order to reduce the heat gains limited its development. Most of the research done up-to-date has focused in the development of correlations and numerical models to determine the effective temperature of the sky and/or the emissivity of the sky [9–12], in the search of selective materials suitable for the dissipation of radiation at certain wavelengths [13–16] and in the evaluation of some specific radiative cooling devices [17–20].

Etzion and Erell [21] highlighted as one of the limitations for the potential of radiative cooling the effect of ambient air on the radiative surface. The cooling potential of the surface allows reaching temperatures much lower than the ambient ones; however, the heat transfer by convection from the ambient air to the radiative cooler reduces its potential. Although different covers transparent to thermal radiation have been studied, there are still some thermal gains that reduce the potential of radiative cooling.

Bathgate and Bosi [22] determined the potential of a radiative cooling device (based on the optical properties of the materials) for different materials and radiator temperatures. They observed that certain selective materials achieved higher power (even doubling it) than using no selective material (black body).

More recently, significant developments have been achieved in the field of materials capable to produce radiative cooling during both night and daytime. In 2013, Rephaeli et al. were the first ones to develop such a material [23,24]. Later on, other materials were developed with similar properties [25–29]. This demonstrates the huge interest and potential of radiative cooling as a renewable technology.

Even with the great research effort done [30], radiative cooling is not a technology mature enough. No commercial device has reached the market yet. The main drawback is its low available cooling power density (between 20 and 80 W/m^2) [31], with peak values of 120 W/m^2 [32] or even higher with new metamaterials (199 W/m^2 in [33]). Therefore, improvements are needed to make radiative cooling feasible. A potential improvement is the coupling of radiative cooling and solar thermal collection in a single device. This new concept will be able to produce both heat and cold, thus improving its feasibility to reach the market. Despite that these two technologies use different types of radiation (different wavelengths), it is possible to couple them as they are not used at the same time, so there is no interference between them; solar collection works during sunlight hours whereas radiative cooling is more effective at night.

Little research has been done in the combination of both solar collection and radiative cooling in a single device, and most of them only characterized the heat produced by a radiative cooler, but did not intend to design and evaluate a device suitable for both functions. Errel and Etsion identified some

of the main differences between a solar collector and a radiative cooler [18]. They highlighted, apart from the cover material, that the radiative cooler needs a pump to circulate the fluid, while the solar collector can in some cases rely on the thermosiphon effect. On the other hand, the effects of convective heat transfer in a solar collector are always negative, since the fluid is always warmer than the ambient. This is not always the case for the radiative cooler, since the air can be used as a cold source during some moments during the night. Finally, they also highlighted that the geometry pipe-fin of a solar collector is not necessarily the best one for a radiative cooler, as they demonstrated numerically.

Erell and Etzion [34] in 1996 used a radiative cooler to perform some experiments under winter conditions to produce heat. Results showed the capacity of the device to produce heat, considering that the system was designed to produce cold and that it had no cover. The main limitation is that, although radiative cooling devices are very similar in shape as solar collectors, their behavior is completely opposed. While the solar collector operates during the sunlight hours to collect shortwave radiation, the radiative cooler operates during night time emitting longwave radiation. This difference in the radiation wavelength means that conventional covers used in solar collectors are not suitable for radiative cooling (since they do not allow longwave radiation to pass through). This and other limitations found by [34] are nowadays of great interest due to the advances in material development and heat transfer optimization. Similar experiments were done more recently by Hosseinzadeh and Taherian [35] and by Xu et al. [36]. However, in all the studies, no cover was used, dramatically limiting the efficiency of the device.

Vall et al. [37] studied the potential of a new concept consisting of combining solar collection and radiative cooling to partially cover the DHW and cooling demands for different typologies of buildings located in different climates. The new concept showed suitability in some of the studied cities with C (temperate) and D (continental) climates in residential and tertiary buildings.

As stated before, new materials have been recently developed for day-long radiative cooling. However, these materials still present the limitation that they do not allow solar collection at the same time. In 2015, Hu et al. [38] developed a spectral selectivity surface suitable for both solar collection and radiative cooling. The new surface, the TPET, presents high absorptivity/emissivity in both the solar radiation and atmospheric window bands. However, this material will also emit in the atmospheric window band during solar radiation collection, which can diminish the heat collection. Moreover, Hu et al. did not consider the radiative properties of the cover of the solar collector/radiative cooler, using polyethylene as cover, which will reduce the efficiency during solar collection mode due to the high emissivity in the near-infrared wavelength [39].

Thus, a research gap is found in the lack of a technology capable of producing both solar collection heating and radiative cooling (RCE).

In this paper, the new concept of combining radiative cooling and solar thermal collection, which is mentioned as Radiative Collector and Emitter (RCE), is presented and experimentally tested. The new concept relies on an adaptive cover that uses different material properties for each functionality: radiative cooling and solar thermal collection. The adaptive cover will provide high spectral transmittance in the solar radiation band and very low spectral transmittance in the infrared band during the solar collection mode, and high spectral transmittance in the atmospheric window wavelength during radiative cooling mode. This innovation will result in a novel approach, based on the adaptive cover and not the collecting/radiating surface, to combine radiative cooling and solar heating.

The purpose of this research and its main novelty is to prove experimentally, for the first time, the RCE concept through the idea of an adaptive cover, which uses different material properties for each functionality: radiative cooling and solar thermal collection. This will contribute to taking the first step in its potential introduction to the market.

2. Experimental Setup

The experimental setup consisted of a solar collector, a radiative cooler, 2 water tanks, a water pump, 6 temperature sensors, 2 flow meters, a pyrgeometer and the control and data acquisition systems. The acquisition data equipment consisted of a data logger (model DIN DL-01-CPU), connected to the adapter data logger-computer (model AC-250). The computer software to compile the data was STEP TCS-01. The solar collector used was model FUJI-P. It was a 2 m × 1 m × 80 mm aluminum frame collector, with a transparent 3 mm glass and 30 mm glass-wool back insulation. The collector has 8 cooper pipes of 8 mm internal diameter and 0.6 mm thick. In a similar way, radiative cooler is in fact a modified version of the same solar collector (FUJI-P), having replaced the glass screen by a 0.6 mm thick polyethylene (PE) film and having painted the surface of the radiator with black paint in order to adapt it to the required characteristics of radiative cooling mode (Figure 1). They were located one next to the other, on the horizontal plane.

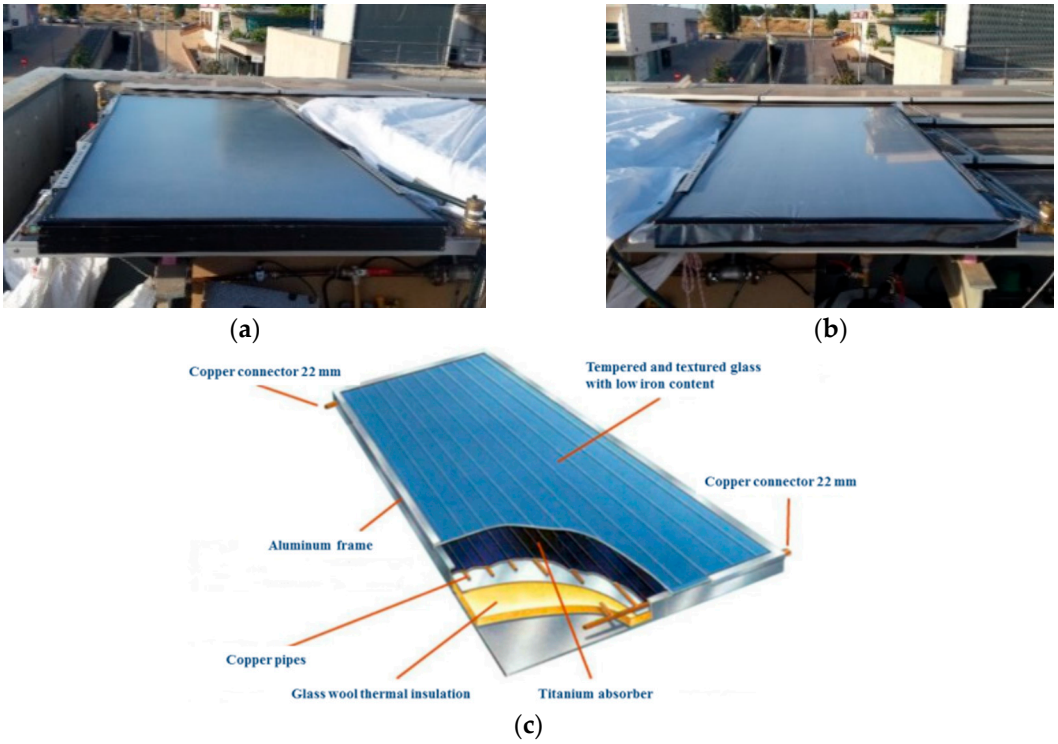

Figure 1. (**a**) Solar collector; (**b**) modified solar collector used as a radiative cooling device; (**c**) Structure of the solar collector FUJI-P (adapted from manufacturer's technical data [40]).

For the sake of simplification, two separate devices were used instead of a single RCE device. This was sufficient to provide accurate data for concept validation, which was the main objective of this research. Four temperature sensors (Pt-100, with an accuracy of ±0.045 °C) were used to monitor the inlet and outlet water temperature of the solar collector and the radiative cooling device. Water flow rates were monitored using a flowmeter for the operation under solar collection mode (Badger Meter-Primo Advanced, 0.25% accuracy), and a flowmeter for the radiative cooling mode (Schmidt Mess-SDNC 503 GA-20, 4% accuracy). Weather data was extracted from a nearby weather station, with the exception of the incoming infrared radiation, which was measured using a pyrgeometer on-site (LP PIRG 01-DeltaOhm, 5% accuracy). All the data from the experiment were registered and recorded at a time-frequency resolution of 1 min. A sketch of the experimental setup is presented in Figure 2.

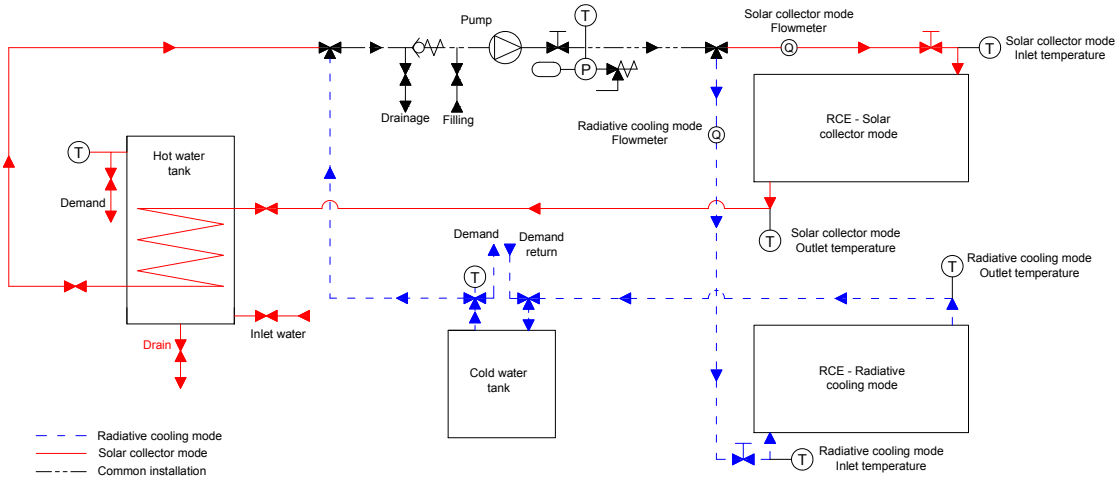

Figure 2. Sketch of the experimental setup.

The film used for the radiative cooler was chosen among different kinds of plastic foils, namely polymethylmethacrylate (PMMA), low-density polyethylene (PELD) and high-density polyethylene (PEHD). Their optical properties were analyzed in the whole spectrum of solar and IR radiations. Three different spectrophotometers were used to cover the UV-vis, the near IR and the far IR spectrum ranges. They were the UV Analytikjena specord 210, the Foss NIR XDS Rapid Content Analyzer and the Jasco FT-IR 6300 series, respectively. PELD film was finally chosen, as it was the most transparent in the infrared band of the electromagnetic radiation. Table 1 shows the resulting mean transmittance in the three measured spectrum ranges for the selected PELD film.

Table 1. Measured mean transmittance for the selected low-density polyethylene (PELD) film.

	UV–Vis	NIR	FT-IR
Range	(0.19–1.1 μm)	(0.4–2.5 μm)	(2.5–15.5 μm)
Mean Transmittance	0.88	0.84	0.98

3. Methodology

3.1. Description of the Experimental Campaign

Experiments were performed for several days combining solar collection mode (from 8.00 to 20.00 h) and radiative cooling mode (from 21.00 to 7.00 h). The experiments were performed during the summer period in Lleida (Dry Mediterranean Continental climate). Specifically, the experimental campaign consisted of two periods; the first one from 26th to 28th July 2017 and the second one from 31st July to 4th August 2017.

The tests were always performed in the same way. Early in the morning, several valves were set to the solar collection mode and the pump was started, so that the water in the secondary circuit, initially in thermal equilibrium with the ambient, could circulate through the RCE and heat up. This water flowed then through the internal heating coil of the hot tank, heating up the water in the tank, which was as well at ambient temperature at the beginning. All the experimental variables were monitored and registered every minute in the data logger. The cloudiness of the sky was observed visually along the day, together with the information about clouds on the online local weather station. After sunset, the set of valves was changed to radiative cooling mode, and then water in the cold tank, initially at ambient temperature, was circulated directly to the RCE, starting the cooling process thanks to the radiative heat transfer to the night sky. As cooling powers are much lower than the heating powers during the day, to prevent heat losses and maximize the cold output, only a primary circuit was used between the cold water tank and the RCE. The water flowrates were kept constant during each test,

although some fluctuations due to the pump operation were observed along the day, with maximum deviations of 25% with respect to the average value (see Table 2). In the second period, the flow rate at night was reduced to about 60% of the daily value to increase the inlet–outlet temperature difference and reduce in that way the uncertainty of the calculated cooling power. The tested range of flow rates was 0.5–1.9 L/min.

Table 2. Operating characteristics of the testing days.

	Date/Hour of Test	Test Label	Clear or Cloudy	Average Volumetric Flow Rate (L/min)
First period	26/07/17 (13:00–20:00)	Day 1.1	Clear	1.36 ± 0.07
	26/07/17 (21:00)–27/07/17 (7:00)	Night 1.1	Clear	1.30 ± 0.02
	27/07/17 (8:00–20:00)	Day 1.2	Clear	1.25 ± 0.2
	27/07/17 (21:00)–28/07/17 (7:00)	Night 1.2	Clear	1.29 ± 0.02
	28/07/17 (8:00–18:00)	Day 1.3	Clear	1.89 ± 0.51
Second period	31/07/17 (8:30–20:00)	Day 2.1	Clear	1.42 ± 0.1
	31/07/17 (21:00)–01/08/17 (7:00)	Night 2.1	Clear	0.63 ± 0.01
	01/08/17 (8:00–20:00)	Day 2.2	Cloudy	1.34 ± 0.14
	01/08/17 (21:00)–02/08/17 (7:00)	Night 2.2	Cloudy	0.56 ± 0.01
	02/08/17 (8:00–20:00)	Day 2.3	Cloudy	1.36 ± 0.09
	02/08/17 (21:00)–03/08/17 (7:00)	Night 2.3	Cloudy	0.57 ± 0.01
	03/08/17 (8:00–20:00)	Day 2.4	Clear	1.34 ± 0.15
	03/08/17 (21:00)–04/08/17 (7:00)	Night 2.4	Clear	0.52 ± 0.02

During the cooling mode, the hot water tank was discharged to ambient temperature using an air–water fin heat exchanger. The same process was used to discharge the cold stored during the night in the cold tank.

The first testing period turned out to be a clear sky period, while the second one combined clear and cloudy days. The details of the testing days, including the operating dates and hours, the day labels and the flow rates used are presented in Table 2.

3.2. Determination of Performance Parameters

To evaluate the performance of the RCE, production rates for both solar collection and radiative cooling were calculated (Equation (1)), as well as efficiencies (Equations (2) and (3)).

$$\dot{q} = v \times \rho \times c_p \times \Delta T \tag{1}$$

where:

$\dot{q}$ is the power of the device (W).
v is the volumetric flow rate (m^3/s).
ρ is the density of the fluid (kg/m^3).
c_p is the heat capacity of the fluid (J/kg·K).
ΔT is the temperature difference between inlet flow T_{in} and outlet flow T_{out} (K).
Solar Collection efficiency:

$$\eta_{sc} = \frac{\int \dot{q}_{sc} dt}{A \int I dt} \tag{2}$$

where:

η_{sc} is the solar collection efficiency (-).
$\dot{q}_{sc}$ is the power of the device in Solar Collector (SC) mode (W).
A is the collector area (m^2).
I is the Solar Irradiation; in this case, Global Horizontal Solar Irradiation (W/m^2).

Radiative Cooling efficiency: The efficiency for the radiative cooling mode is based on the one presented in [41] but considering the surface temperature of the RCE device instead of ambient temperature to determine the infrared radiation emitted in the effective outgoing infrared radiation term.

$$\eta_{rc} = \frac{\int \dot{q}_{rc} dt}{A \int R \, dt} \tag{3}$$

where:

η_{rc} is the radiative cooling efficiency (-).

$\dot{q}_{rc}$ is the power of the device in Radiative Cooling (RC) mode (W).

A is the collector area (m^2).

R is the effective outgoing infrared radiation (W/m^2).

The value of R is determined as the difference between the infrared radiation emitted by the radiative cooler surface ($R_{\uparrow}$) and the infrared radiation from the atmosphere (sky) absorbed by this surface ($R_{\downarrow}$):

$$R = R_{\uparrow} - R_{\downarrow} = \left(\varepsilon \times \sigma \times T_{rc}^4 \; - \; R_{\downarrow}\right) \tag{4}$$

where:

$R_{\downarrow}$ is the Incoming Radiation (measured on-site) (W/m^2).

$R_{\uparrow}$ is the infrared radiation emitted by the radiative cooler surface (W/m^2).

ε is the ideal radiator emissivity/absorptivity, in this case 1 (-).

σ is the Stefan–Boltzmann constant, 5.67×10^{-8} (W/m^2 K^4).

T_{rc} is the temperature of the radiator (average inlet/outlet) (K).

This radiative cooling net balance of the surface, R, is considered the maximum potential for radiative cooling of the RCE, and should be compared with the actual cooling power that is transferred to the water, $\dot{q}_{rc}$, to evaluate the radiative cooler efficiency during the night (Equation (3)).

The uncertainty of the above presented experimental parameters (Equations (1)–(3)) have been calculated as a function of the direct measured variables (namely, inlet water temperature T_{in}, outlet water temperature T_{out}, volumetric flow rate υ, solar irradiation I and incoming IR radiation $R_{\downarrow}$) and their associated accuracy. The heat capacity c_p and the density ρ values for water are taken from the literature at the average RCE temperature. Applying the standard method for uncertainty propagation [42], the calculated uncertainty for heating power (day), cooling power (night), solar collector efficiency and radiative cooler efficiency are 3%, 8%, 3% and 20%, respectively. Special care was taken in the selection of instruments with the lowest uncertainties possible, as the low radiative cooling powers at nights made them more critical to finally obtain reasonable uncertainties.

4. Results and Discussion

In the following section direct measurement and calculated parameters for the RCE testing periods are presented and discussed.

4.1. Direct Measurements and Testing Observations

During the first period, the meteorology was stable with all-day clear and sunshine. The outdoor temperature oscillated from 19 to 40 °C, with Global Horizontal Irradiation (GHI) peak values up to 960 W/m^2, average values of 670 W/m^2 and Incoming Infrared Radiation average values of 340 W/m^2. In the second period, the meteorology was stable with some cloudy days and the outdoor temperature oscillated from 23 to 42 °C, with GHI peak values up to 935 W/m^2, a GHI average value of 539 W/m^2 and Incoming Infrared Radiation average values of 355 W/m^2.

In the first testing period, mainly under clear sky conditions, the RCE was capable to produce heat, reaching maximum outlet temperature values of 64 °C (Figure 3), achieving average temperature differences between the outlet water (T_{out}) and the ambient (T_{amb}) around 17–22 °C (Table 2). In the second period, with both cloudy and clear days, the RCE produced heat as well, reaching maximum

outlet temperature values of 67 °C for the two clear days, but lower values the other two days (47–60 °C). The average temperature differences between the outlet water and the ambient in this period were around 8–14 °C (Table 2).

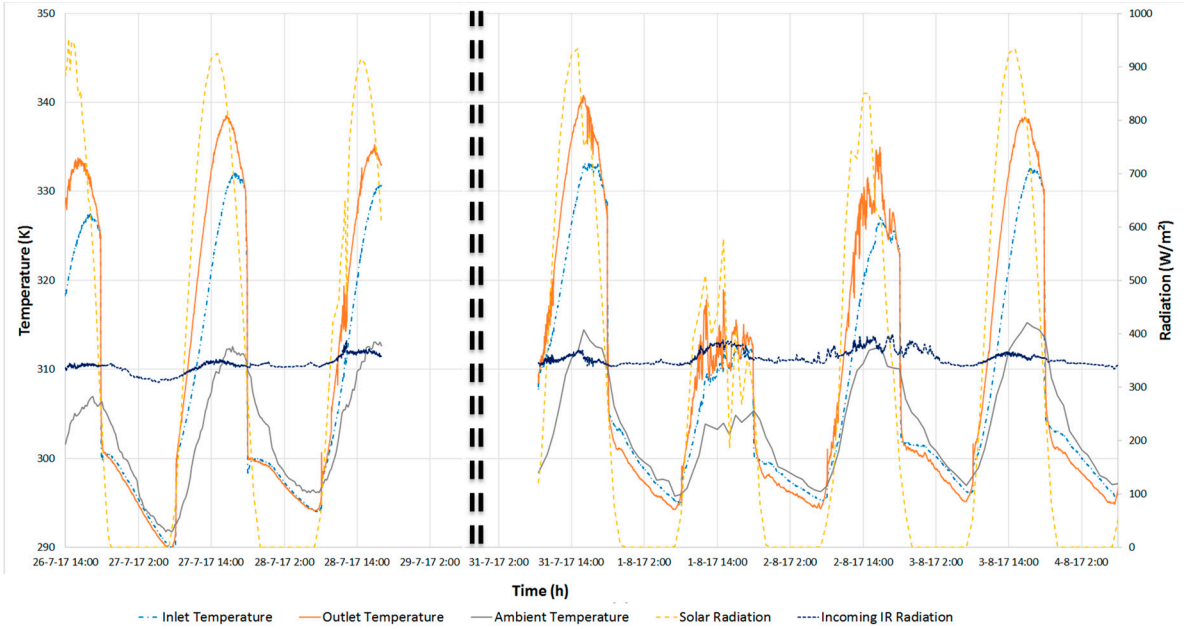

Figure 3. Experimental results of the Radiative Collector and Emitter (RCE) concept.

The measured incoming sky IR radiation remained very stable along the two test periods, in a range 310–400 W/m^2, with slightly higher values during the days and in cloudy periods, and more oscillations in cloudy periods (Figure 3).

On the other hand, the RCE also showed the capability to produce cold water, reaching minimum outlet water temperatures close to 16 °C in the first period and of 20 °C in the second one (Figure 3), with average temperature differences between the outlet water and ambient around 2–3 °C (Table 2).

Apart from measured data, other empirical details were observed. In some occasions, the radiative emitter presented dew or water moisture attached to the inner part of the plastic foil. This phenomenon was observed during the morning inspection and it was not possible to determine when it occurs as well as the effects on the performance. Despite the effects were not quantified, it reduces the performance of the system because the water film becomes the radiating surface [43]. This effect blocks the direct contact between the surface of the radiator and the sky.

4.2. Heating and Cooling Powers for RCE

Figure 4 shows the calculated heating and cooling power produced by the RCE during the two testing periods (see Equation (1)). Note that for the sake of clarity the cooling power scale (right vertical axis) is one order of magnitude smaller than the heating power scale (left vertical axis) and the absolute value is used for cooling, skipping the negative sign. In the first clear sky period average heating powers of 290–315 W/m^2 are achieved, with peak values above 500 W/m^2, whereas in the second period, the average heating powers are smaller (range 120–290 W/m^2), with a peak of 539 W/m^2 in Day 6 (Figure 4 and Table 3). Daily average solar collector efficiencies of 0.43–0.49 are achieved in the first period, while in the second period they are slightly lower, in the range 0.34–0.46 (Table 3). Regarding the cooling power at nights, average values between 13–34 W/m^2 were achieved, with peak powers above 46 W/m^2 on Day 4 (Figure 4 and Table 3). Average radiative cooling efficiencies in the range 0.12–0.32 were obtained (Table 3).

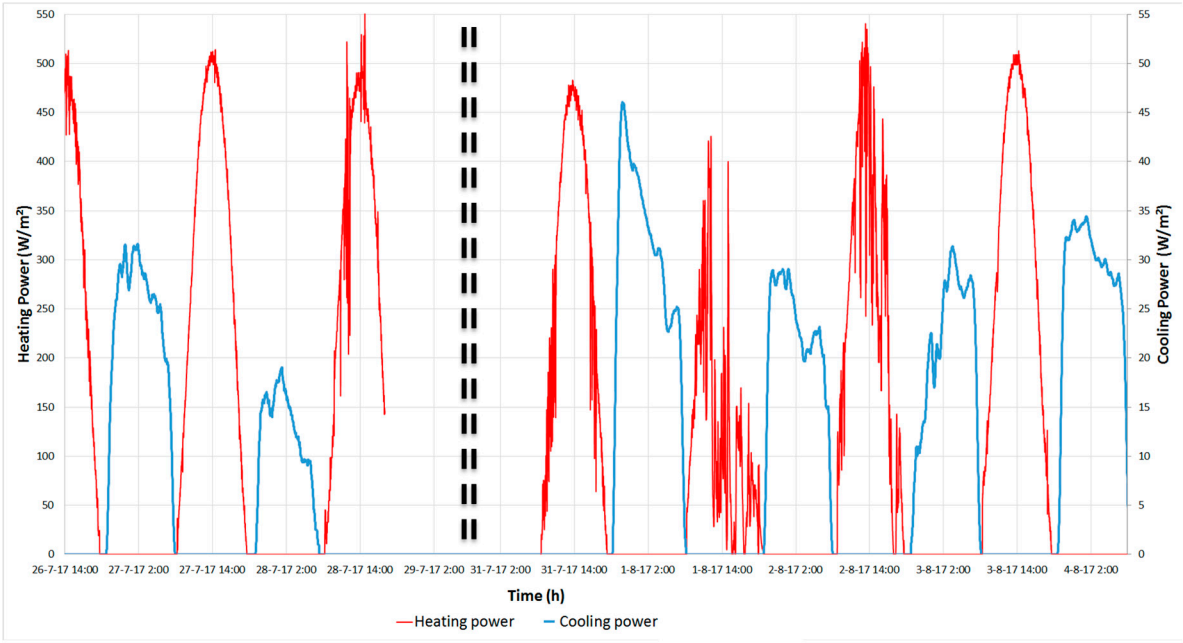

Figure 4. Available heating and cooling power from the RCE concept.

Table 3. Average and peak power produced, average temperature diffrence and average efficiency by the RCE for both heat and cold production.

	Heating Power, $\dot{q}_{sc}$ (W/m^2)		Cooling Power, $\dot{q}_{rc}$ (W/m^2)		Average ($T_{out} - T_{amb}$) (K)		Average Efficiency (%)	
Test Period	**Average**	**Peak**	**Average**	**Peak**	**Heating**	**Cooling**	**Heating, η_{sc}**	**Cooling, η_{rc}**
Day 1.1	313.3	545.5	-	-	24.98	-	43	-
Night 1.1	-	-	26.04	36.3	-	−2.14	-	24
Day 1.2	293.5	513.8	-	-	19.68	-	46	-
Night 1.2	-	-	12.63	22.5	-	−2.68	-	12
Day 1.3	310.7	583.3	-	-	13.84	-	49	-
Day 2.1	265.7	482.9	-	-	20.65	-	42	-
Night 2.1	-	-	33.35	48.5	-	−2.47	-	32
Day 2.2	122.9	425.7	-	-	8.16	-	34	-
Night 2.2	-	-	23.84	31.6	-	−2.56	-	26
Day 2.3	238.6	538.5	-	-	12.95	-	46	-
Night 2.3	-	-	22.69	33.9	-	−2.62	-	24
Day 2.4	293.0	512.7	-	-	15.71	-	46	-
Night 2.4	-		30.64	36.2	-	−3.44	-	28

4.3. Maximum Potential for Cooling

Figure 5 shows the calculated effective IR radiation from the RCE to the sky, which gives the maximum potential for cooling for the RCE. The incoming IR radiation measured by the pyrgeometer and the calculated outgoing IR radiation from the RCE surface (see Equation (4)) are included as well. It is interesting to notice that the potential for cooling increases a lot in the RCE during the day. This is due to the fact that the RCE is working as a solar collector at that time, and the temperature of the absorber/emitter surface is quite high (40–70 °C) and, thus, the capacity to irradiate to the sky increases above 350 W/m^2 of cooling power. However, the glass cover blocks this potential IR radiation to the sky. The importance of the proposed adaptive cover is highlighted here also for the heating operating mode. If only the PE film was used as cover, this cooling power would be mostly radiated to the sky through the PE film and the solar collector efficiency of the RCE would substantially decrease.

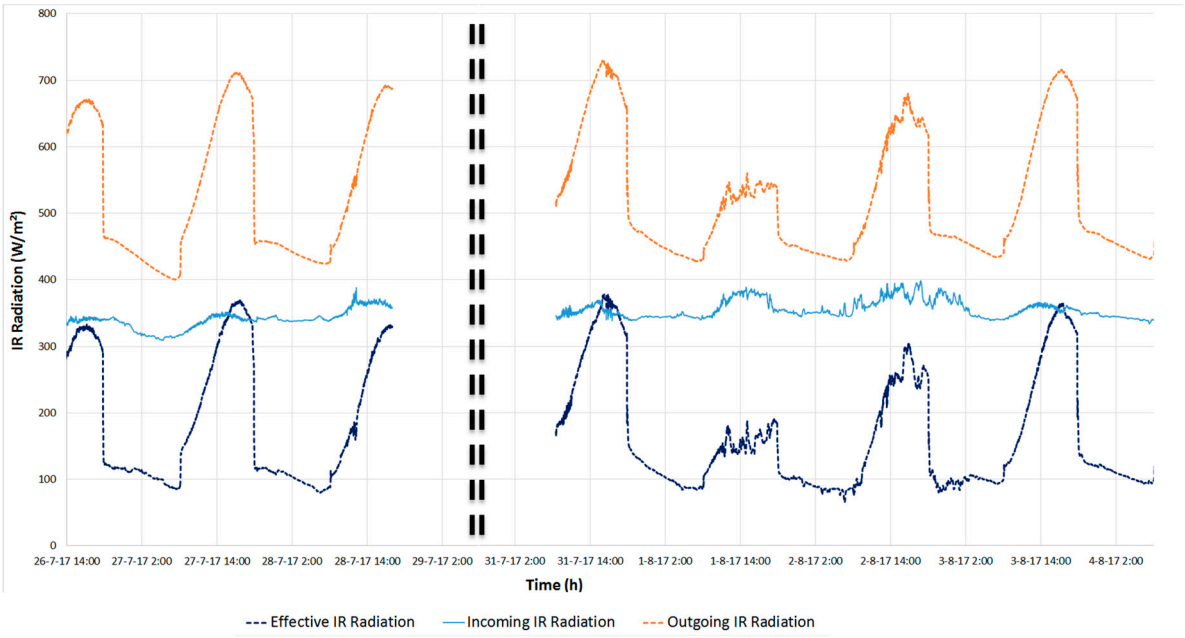

Figure 5. Incoming, outgoing and net effective radiation of the RCE concept.

5. Conclusions

The present research designed, constructed and analyzed experimentally the concept of the combined renewable production of heating and cooling via thermal collection and sky radiative cooling in a single device, the Radiative Collector and Emitter (RCE) device. It proved the concept and showed the potential to be introduced in buildings as an active system for heating and cooling. The results demonstrate the potential of the RCE concept to heat up water during daylight hours and to cool down water during the night.

Along the tested days, the RCE device produced peak heating power values up to 583 W/m^2 during the day, with average efficiencies up to 49%. During the night the RCE achieved peak cooling powers of 33 W/m^2, with average cooling efficiencies up to 32%. When compared to other cooling technologies such as electrically driven compression water chillers, RCE is not able to provide the same low temperature levels (7–12 °C) or efficiencies (SEER of 2–5). It is important to bear in mind that chillers and other existing cooling technologies consume non-renewable primary energy whereas the RCE is driven by renewable primary energy. When primary energy is considered, RCE average cooling efficiencies are in the same order of magnitude than those of electrically driven compression water chillers (80%–100%, based on a Primary Energy Factor of 2.5 [44]). Thus, the wise decision in a building with both technologies would be to give priority to the RCE, even with a low performance, and then complement the demand and/or temperature level shortcomings with the compression chillers.

Although improvements are required in order to maximize the cold production and reach useful temperature levels, this first RCE prototype has proven the concept of cooling down water below ambient temperature by the use of sky night radiation, while heating up water during the day.

Special attention was put on the radiative cooling mode. Even if it was not the best season for radiative cooling mode, with shorter periods of nighttime, it is in summer when it makes sense to produce cold. The cold produced during the night can be used either as a direct cooling source or as a heat sink for other cooling technologies (such as heat pumps) in order to improve its efficiency, thus reducing the use of non-renewable energies. However, further improvements are required to take full advantage of this new concept.

A negative effect was observed during experimental testing. The formation of dew was on both sides of the cover, but especially in the inner side. The dew on the inner (and outer) side of the cover can be a problem for the performance of the system, especially in humid climates. However, some

solutions such as creating a vacuum between the radiator surface and the cover can eliminate or mitigate its effects.

Future research will address the first prototype of the single RCE device, with a practical solution for an automatically controlled adaptive cover.

Author Contributions: Conceptualization, S.V., A.C. and C.S.; methodology, A.C. and S.V.; formal analysis, S.V. and M.M.; investigation, S.V. and C.S.; data curation, S.V. and M.M.; writing—S.V.; writing—review and editing, M.M., A.C. and C.S.; visualization, S.V. and M.M.; supervision, A.C.; project administration, A.C.; funding acquisition, A.C. All authors have read and agreed to the published version of the manuscript.

Funding: This research was funded by the Oficina de Desenvolupament i Cooperació (ODEC), the Catalan Government (AGAUR–Generalitat de Catalunya) under grant agreement 2017 SGR 659, the Spanish government (Ministerio de Ciencia, Innovación y Universidades) under grant agreement RTI2018-097669-A-I00.

Acknowledgments: The authors would like to thank the Oficina de Desenvolupament i Cooperació de la Universitat de Lleida for the project grant. The authors would like to thank the Catalan Government for the quality accreditation given to their research group (2017 SGR 659). The work was partially funded by the Spanish government under grant agreement RTI2018-097669-A-I00 (Ministerio de Ciencia, Innovación y Universidades). Sergi Vall would like to thank the Secretaria d'Universitats i Recerca del Departament d'Economia i Coneixement de la Generalitat de Catalunya for the research fellowship.

Conflicts of Interest: The authors declare no conflicts of interest. The funders had no role in the design of the study; in the collection, analyses, or interpretation of data; in the writing of the manuscript, or in the decision to publish the results.

References

1. European Parliament. Directive (EU) 2018/844 of the European Parliament and of the Council of 30 May 2018 amending Directive 2010/31/EU on the energy performance of buildings and Directive 2012/27/EU on energy efficiency (Text with EEA relevance). *Off. J. Eur. Union* **2018**, *156*, 75–91. [CrossRef]
2. Kristin, S.; Sverrisson, F.; Appavou, F.; Brown, A.; Epp, B.; Leidreiter, A. *Renewables 2016 Global Status Report*; Ren21: Paris, France, 2016. Available online: https://www.ren21.net/wp-content/uploads/2019/05/REN21_GSR2016_FullReport_en_11.pdf (accessed on 1 June 2018).
3. Hughes, B.R.; Chaudhry, H.N.; Ghani, S.A. A review of sustainable cooling technologies in buildings. *Renew. Sustain. Energy Rev.* **2011**, *15*, 3112–3120. [CrossRef]
4. European Commission. Decision of 1 March 2013 (2013/114/EU) establishing the guidelines for Member States on calculating renewable energy from heat pumps from different heat pump technologies pursuant to Article 5 of Directive 2009/28/EC of the European Parliament and of the. *Off. J. Eur. Union* **2013**, *62*, 27–35.
5. European Parliament. Directive 2009/28/EC of the European Parliament and of the Council of 23 April 2009 on the promotion of the use of energy from renewable sources and amending and subsequently repealing Directives 2001/77/EC and 2003/30/EC. *Off. J. Eur. Union* **2009**, *140*, 16–62. [CrossRef]
6. Hassan, H.Z.; Mohamad, A.A. A review on solar cold production through absorption technology. *Renew. Sustain. Energy Rev.* **2012**, *16*, 5331–5348. [CrossRef]
7. Bell, E.E.; Eisner, L.; Young, J.; Oetjen, R.A. Spectral-Radiance of Sky and Terrain at Wavelengths between 1 and 20 Microns. II. Sky Measurements. *J. Opt. Soc. Am.* **1960**, *50*, 1313–1320. [CrossRef]
8. Zhang, K.; McDowell, T.P.; Kummert, M. Sky Temperature Estimation and Measurement for Longwave Radiation Calculation. In Proceedings of the 15th IBPSA Conf 2017, San Francisco, Ca, USA, 7–9 August 2017. [CrossRef]
9. Swinbank, W.C. Long-wave radiation from clear skies. *Q. J. R. Meteorol. Soc.* **1963**, *89*, 339–348. [CrossRef]
10. Idso, S.B. A Set of Equations for Full Spectrum and 8- to 14 micron and 10.5- to 12.5 micron Thermal Radiation From Cloudless Skies. *Water Resour. Res.* **1981**, *17*, 295–304. [CrossRef]
11. Berdahl, P.; Martin, M. Emissivity of clear skies. *Sol. Energy* **1984**, *32*, 663–664. [CrossRef]
12. Prata, A.J. A new long-wave formula for estimating downward clear-sky radiation at the surface. *Q. J. R. Meteorol. Soc.* **1996**, *122*, 1127–1151. [CrossRef]
13. Catalanotti, S.; Cuomo, V.; Piro, G.; Ruggi, D.; Silvestrini, V.; Troise, G. The radiative cooling of selective surfaces. *Sol. Energy* **1975**, *17*, 83–89. [CrossRef]
14. Granqvist, C.G.; Hjortsberg, A. Radiative cooling to low temperatures: General considerations and application to selectively emitting SiO films. *J. Appl. Phys.* **1981**, *52*, 4205–4220. [CrossRef]

15. Eriksson, T.S.; Lushiku, E.M.; Granqvist, C.G. Materials for radiative cooling to low temperature. *Sol. Energy Mater.* **1984**, *11*, 149–161. [CrossRef]
16. Tazawa, M.; Jin, P.; Tanemura, S. Thin film used to obtain a constant temperature lower than the ambient. *Thin Solid Films* **1996**, *281–282*, 232–234. [CrossRef]
17. Mihalakakou, G.; Ferrante, A.; Lewis, J.O. The cooling potential of a metallic nocturnal radiator. *Energy Build.* **1998**, *28*, 251–256. [CrossRef]
18. Erell, E.; Etzion, Y. Radiative cooling of buildings with flat-plate solar collectors. *Build. Environ.* **2000**, *35*, 297–305. [CrossRef]
19. Sima, J.; Sikula, O.; Kosutova, K.; Plasek, J. Theoretical Evaluation of Night Sky Cooling in the Czech Republic. *Energy Procedia* **2014**, *48*, 645–653. [CrossRef]
20. Bagiorgas, H.S.; Mihalakakou, G. Experimental and theoretical investigation of a nocturnal radiator for space cooling. *Renew. Energy* **2008**, *33*, 1220–1227. [CrossRef]
21. Etzion, Y.; Erell, E. Thermal Storage Mass in Radiative Cooling Systems. *Build. Environ.* **1991**, *26*, 389–394. [CrossRef]
22. Bathgate, S.N.; Bosi, S.G. A robust convection cover material for selective radiative cooling applications. *Sol. Energy Mater. Sol. Cells* **2011**, *95*, 2778–2785. [CrossRef]
23. Rephaeli, E.; Raman, A.P.; Fan, S. Ultrabroadband Photonic Structures To Achieve High-Performance Daytime Radiative Cooling. *Nano Lett.* **2013**, *13*, 1457–1461. [CrossRef] [PubMed]
24. Raman, A.P.; Anoma, M.A.; Zhu, L.; Rephaeli, E.; Fan, S. Passive radiative cooling below ambient air temperature under direct sunlight. *Nature* **2014**, *515*, 540–544. [CrossRef] [PubMed]
25. Huang, Z.; Ruan, X. Nanoparticle embedded double-layer coating for daytime radiative cooling. *Int. J. Heat Mass Transf.* **2017**, *104*, 890–896. [CrossRef]
26. Huang, Y.; Pu, M.; Zhao, Z.; Li, X.; Ma, X.; Luo, X. Broadband metamaterial as an "invisible" radiative cooling coat. *Opt. Commun.* **2018**, *407*, 204–207. [CrossRef]
27. Wu, D.; Liu, C.; Xu, Z.; Liu, Y.; Yu, Z.; Yu, L.; Ye, H. The design of ultra-broadband selective near-perfect absorber based on photonic structures to achieve near-ideal daytime radiative cooling. *Mater. Des.* **2018**, *139*, 104–111. [CrossRef]
28. Yang, P.; Chen, C.; Zhang, Z.M. A dual-layer structure with record-high solar reflectance for daytime radiative cooling. *Sol. Energy* **2018**, *169*, 316–324. [CrossRef]
29. Wong, R.Y.M.; Tso, C.Y.; Chao, C.Y.H.; Huang, B.; Wan, M.P. Ultra-broadband asymmetric transmission metallic gratings for subtropical passive daytime radiative cooling. *Sol. Energy Mater. Sol. Cells* **2018**, *186*, 330–339. [CrossRef]
30. Vall, S.; Castell, A. Radiative cooling as low-grade energy source: A literature review. *Renew. Sustain. Energy Rev.* **2017**, *77*, 1–18. [CrossRef]
31. Cavelius, R.; Isaksson, C.; Perednis, E.; Read, G.E.F. *Passive Cooling Technologies*; Austrian Energy Agency: Vienna, Austria, 2005.
32. Eicker, U.; Dalibard, A. Photovoltaic-thermal collectors for night radiative cooling of buildings. *Sol. Energy* **2011**, *85*, 1322–1335. [CrossRef]
33. Kong, A.; Cai, B.; Shi, P.; Yuan, X. Ultra-broadband all-dielectric metamaterial thermal emitter for passive radiative cooling. *Opt. Express* **2019**, *27*, 30102–30115. [CrossRef]
34. Erell, E.; Etzion, Y. Heating experiments with a radiative cooling system. *Build. Environ.* **1996**, *31*, 509–517. [CrossRef]
35. Hosseinzadeh, E.; Taherian, H. An Experimental and Analytical Study of a Radiative Cooling System with Unglazed Flat Plate Collectors. *Int. J. Green Energy* **2012**, *9*, 766–779. [CrossRef]
36. Xu, X.; Niu, R.; Feng, G. An Experimental and Analytical Study of a Radiative Cooling System with Flat Plate Collectors. *Procedia Eng.* **2015**, *121*, 1574–1581. [CrossRef]
37. Vall, S.; Castell, A.; Medrano, M. Energy Savings Potential of a Novel Radiative Cooling and Solar Thermal Collection Concept in Buildings for Various World Climates. *Energy Technol.* **2018**, *6*, 2200–2209. [CrossRef]
38. Hu, M.; Pei, G.; Li, L.; Zheng, R.; Li, J.; Ji, J. Theoretical and Experimental Study of Spectral Selectivity Surface for Both Solar Heating and Radiative Cooling. *Int. J. Photoenergy* **2015**, *2015*, 807875. [CrossRef]
39. Hu, M.; Pei, G.; Wang, Q.; Li, J.; Wang, Y.; Ji, J. Field test and preliminary analysis of a combined diurnal solar heating and nocturnal radiative cooling system. *Appl. Energy* **2016**, *179*, 899–908. [CrossRef]

40. Fujisol S.S.L. Energías Renovables.—N.d. Available online: https://www.fujisol.com/pdf/ficha-fujip.pdf (accessed on 22 January 2020).
41. Hu, M.; Zhao, B.; Ao, X.; Zhao, P.; Su, Y.; Pei, G. Field investigation of a hybrid photovoltaic-photothermic-radiative cooling system. *Appl. Energy* **2018**, *231*, 288–300. [CrossRef]
42. Taylor, B.N.; Kuyatt, C.E. *Guidelines for Evaluating and Expressing the Uncertainty of NIST Measurement Result*; National Institute of Standards and Technology: Gaithersburg, MD, USA, 1994.
43. Erell, E.; Etzion, Y. A Radiative Cooling System Using Water as a Heat Exchange Medium. *Archit. Sci. Rev.* **1992**, *35*, 39–49. [CrossRef]
44. European Parliament. Directive 2012/27/EU of the European Parliament and of the Council of 25 October 2012 on energy efficiency. *Off. J. Eur. Union Dir.* **2012**, 1–56. [CrossRef]